2017

Theoretical Modelling and Design of Photonic Structures in Zeolite Nanocomposites for Gas Sensing: Part I - Surface Relief Gratings

Dervil Cody
Technological University Dublin, dervil.cody@tudublin.ie

Izabela Naydenova
Technological University of Dublin, izabela.naydenova@tudublin.ie

Recommended Citation

Cody, I. & Naydenova, I. (2017). Theoretical Modelling and Design of Photonic Structures in Zeolite Nanocomposites for Gas Sensing: Part I - Surface Relief Gratings. *Journal of the Optical Society of America*, vol. 34, no. 12, pp. 2110-2119. doi.org/10.1364/JOSAA.34.002110.

Theoretical modelling and design of photonic structures in zeolite nanocomposites for gas sensing: part I - surface relief gratings

D. CODY,[1] I. NAYDENOVA[1*]

[1]*Centre for Industrial and Engineering Optics, School of Physics and Clinical and Optometric Sciences, College of Sciences and Health, Dublin Institute of Technology, Kevin Street, Dublin 8, Ireland.*
**Corresponding author: izabela.naydenova@dit.ie*

Received XX Month XXXX; revised XX Month, XXXX; accepted XX Month XXXX; posted XX Month XXXX (Doc. ID XXXXX); published XX Month XXXX

The suitability of holographic structures fabricated in zeolite nanoparticle-polymer composite materials for gas sensing applications has been investigated. Theoretical modelling of the sensor response (i.e. change in hologram readout due to a change in refractive index modulation or thickness as a result of gas adsorption) of different sensor designs was carried out using Raman-Nath theory and Kogelnik's Couple Wave Theory. The influence of a range of parameters on the sensor response of holographically-recorded surface and volume photonic grating structures has been studied, namely phase difference between the diffracted and probe beam introduced by the grating, grating geometry, thickness, spatial frequency, reconstruction wavelength and zeolite nanoparticle refractive index. From this, the optimum fabrication conditions for both surface and volume holographic gas sensor designs have been identified. Here in part 1, results from theoretical modelling of the influence of design on the sensor response of holographically-inscribed surface relief structures for gas sensing applications is reported.

OCIS codes: *050.0050 Diffraction and gratings; 280.0280 Remote sensing and sensors; 220.0220 Optical design and fabrication*

http://dx.doi.org/

1. INTRODUCTION

Sensors play an indispensable role in achieving environmental sustainability via monitoring of air and water quality. In recent years, the development of chemical vapour and gas sensors has expanded significantly in terms of financial investment and the volume of research being conducted [1-7]. The global market for gas sensors is expected to reach a value of $ 2.5 billion in 2020 [7]. This increasing demand is partly due to new regulatory initiatives which are placing increasing legislative pressure on industry to monitor levels of potentially hazardous chemicals and gases in the workplace. The level of toxic fumes from waste products must also be monitored in order to minimise damage to the environment. The range of fields requiring gas sensing technologies is large and varied, incorporating the process and petrochemical industries, atmospheric monitoring, and breath diagnostics.

Optical sensors operate via a quantifiable and/or visible modification or modulation to some characteristic of light incident on the sensor due to an external influence. Optical sensors have advantages over other sensor types such as semiconductor and electrochemical sensors due to their fast response, relatively low cost, and immunity to interference from electromagnetic fields, as well as allowing for label-free, in-situ, real-time measurements [1]. Holographic sensors are photonic structures which offer additional advantages: they are light-weight, suitable for mass production and can be fabricated to produce visible 3D images. Holographic sensors can be designed to provide an immediate visual indication in the presence of pollutants i.e. a colour change, or via a digital readout [8].

A holographic diffraction grating may act as a sensor when, under exposure to some analyte, a quantifiable change in the optical properties of the grating occurs. For a transmission mode holographic sensor, surface or volume, the analyte is detected via a change in the diffraction efficiency and/or diffraction angle of the holographic grating due to modification of the grating thickness (i.e. a change in the grating fringe spacing) or refractive index modulation. For a reflection mode holographic sensor, a shift in the diffracted light peak wavelength, intensity and/or angle of the reconstructed hologram is observed due to a change in hologram refractive index modulation or hologram swelling/shrinkage i.e. thickness change in the presence of the analyte. The sensitivity of the holographic sensor will depend largely on the extent to which the refractive index of the material changes, and on the ability of the material to undergo dimensional changes by shrinking/expanding. In this work, systematic theoretical modelling of the sensor response of different holographic structures has been carried out for the first time in order to identify the optimum design for a highly sensitive holographic gas sensor based on surface and volume photonic structures.

The development of holographic sensors is an active research area. In 1999, Lowe et al, demonstrated that a poly(hydroxyethyl methacrylate)-based reflection hologram could successfully be used as a liquid-phase alcohol sensor by monitoring the shift in the peak wavelength of the reconstructed hologram due to hologram swelling in the presence of the alcohol [9]. This same principle has been exploited extensively to develop polymer-based holographic sensors for many other liquid-based analytes including glucose [10], divalent metal ions [11] and pH [12], as well as to quantify environmental parameters such as temperature [13] and pressure [14, 15]. In 2008, Naydenova et al reported the use of a photopolymer-based reflection hologram to produce a visual indication of environmental humidity i.e. detection of water vapour [16] and later zeolite doped holographic structures sensitive to toluene [17] and isopropanol [8] were reported. The incorporation of zeolites for improved holographic device sensitivity to organic vapours such as acetone [18] and ethanol [19] was subsequently investigated by Yu et al. Both transmission mode [8] and reflection mode [20] polymer-based holograms have been developed for the real-time detection of gaseous volatile organic compounds (VOCs). Hsiao et al report on the holographic fabrication of porous polymer-based organic solvent vapour sensors for acetone, chloroform and toluene which operate via a change in the peak reflective wavelength of the resulting photonic bandgap structures [21]. The use of surface holographic structures which are inscribed by interferometric lithography as an alternative to volume holographic structures have also been reported recently. Testosterone sensors have been developed in holographic molecularly imprinted polymer (MIP) films using interference photolithography [22, 23]. Molecularly imprinted polymer is prepared by templating at the molecular level. These polymer materials require a very high degree of cross-linking in order to obtain enough rigidity in the imprinted cavities in the polymer matrix to maintain specificity. However, this requirement conflicts with the fundamental need for flexibility required for obtaining significant change in the structure upon binding of the target analyte which is necessary for high sensitivity. The use of another type of holographically recorded surface structure, known as an Aztec grating [24-27] in holographic sensing was first proposed in [28]. Theoretical and experimental studies of the properties of sensors based on this structure have been recently published [29]. The main difference in this approach is that the sensor response is caused by a change in the refractive index of the functionalising material, and not due to dimensional changes of the functionalising layer upon binding of the analyte, since the reflection happens from a fixed structure. A relative humidity sensor based on a 2.5-dimensional honeycomb pyramidal surface relief grating, or Aztec hologram, has been demonstrated in [30]. The embossed surface structure is functionalised for water vapour via coating with hydrophilic materials such as polyvinyl alcohol and glycerol.

While several theoretical models have been put forward in recent years to describe the operation of holographic sensors [8, 31, 32], there has been limited discussion on the optimum physical structure or design of a hologram in order to maximise the sensor performance. Sensors must meet several requirements including high sensitivity, fast response, selectivity, and reversibility/irreversibility depending on the application. Ideally, a sensor will detect and quickly respond to low concentrations of an analyte present in its environment. In addition to material properties, the physical structure of the hologram has significant impact on the extent of the response of the holographic sensor i.e. whether it is a transmission or reflection hologram, a surface or volume hologram. In addition to geometry there are many additional parameters such as refractive index modulation, grating period, thickness/surface relief amplitude and reconstruction wavelength which can be optimised to maximise the achievable modulation in the optical properties of the sensor as a result of a change in refractive index modulation and/or hologram thickness in the presence of the target analyte.

In this work, the influence of the design of surface relief and volume holographic structures on the sensor response for gas sensing applications has been theoretically investigated for the first time. Part 1 focuses on surface relief gratings (SRGs) which are holographically-inscribed in polymer media such as photopolymers and photoresists, and then functionalised with zeolite nanoparticles. Zeolite nanoparticles are an attractive option for functionalisation of holographic gas sensors due to their controllable porosity which allows for increased selective adsorption of gas molecules. The physical and chemical properties of the zeolites can be tuned to allow for pairing with specific gaseous analytes, thereby allowing for sensor selectivity [33-35]. The influence of sensor design on the sensor response has been modelled for a range of parameters including phase difference between the probe and diffracted beam introduced by the grating, grating period, surface relief amplitude, reconstruction wavelength and the optical properties of the zeolite nanoparticles. The optimum design for an SRG-based gas sensor has been identified, and the advantages and disadvantages to this approach are discussed.

2. THEORY

A. Principle of operation of SRG sensors

The surface of a photosensitive medium may be holographically patterned for a range of applications including sensing via illumination with an interference pattern of light of an appropriate wavelength [36, 37]. The structure of the holographic pattern (or SRG) may be defined by the aspect ratio, which is the ratio of surface relief amplitude to the grating period. Among the family of materials available for fabricating such holographic structures, photopolymers and photoresists perhaps offer the greatest control over grating period and surface relief amplitude.

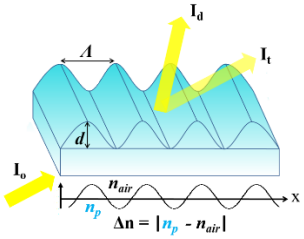

Fig. 1. SRG with thickness d and period Λ.

In photopolymers, the surface relief profile is formed due to polymerisation of illuminated regions, resulting in a localised change in the materials properties. Surface analysis of an acrylamide-based photopolymer shows that the surface relief peaks coincide with the illuminated (i.e. polymerised) fringe regions due to the diffusion of acrylamide monomer into the illuminated regions during holographic recording [38]. Surface relief amplitudes of up to 4 μm are reported for a grating spatial frequency of 16 lines/mm [39]. This drops to 250 nm as the spatial frequency is increased to 500 lines/mm. In photoresist media, illuminated regions become soluble or insoluble to a chemical developer, depending on whether the photoresist is classified as positive or negative respectively. Photoresists have long been utilized for their ability to achieve large surface modulations at low grating periods. Surface relief structures with amplitudes of up to 800 nm can be achieved via holographic methods for a spatial frequency of 5000 lines/mm [40].These photoresist gratings can also be used as masks to produce surface relief structures in other polymer materials such as MIPs [21, 41, 42]. In both photopolymers and photoresists, the

maximum achievable surface relief amplitude decreases with a reduction in the grating period. While photoresists offer greater surface relief amplitudes in comparison to photopolymers, photoresists require a chemical post-processing step which is undesirable for large-scale device fabrication.

A schematic of a SRG with surface amplitude d and period Λ is shown in fig. 1. The initial refractive index modulation, Δn, of the surface grating is calculated from the difference between the refractive index of the material n_p and that of air. Any change in the value of Δn of the grating will vary the phase difference (φ) between the beams propagating in directions along the zero (I_t) and the higher orders (I_d) of diffraction from the grating when illuminated with a probe beam (I_o), measurable as a change in the grating diffraction efficiency η, defined here as the ratio of I_d to I_o. SRGs are an attractive option for gas sensing as, unlike for volume grating-based sensors, the gas molecules do not have to permeate the volume of the layer (with thickness typically tens of micrometers) and can readily interact with the grating on the layer surface (typically less than a micrometer), potentially increasing the sensor sensitivity, response time and reversibility.

1. Zeolite-coated SRGs for gas sensing

The method of functionalisation of the holographic sensor is an important consideration, as the physical and optical properties of the functionalising material will influence the sensor design and sensitivity. Zeolite nanoparticles are defined as crystalline nano- and mesoporous materials with 3D framework structures that form regular and uniform pores and channels [34]. They can be synthesised with different chemical compositions and frameworks which allows for a wide variety of materials; currently more than 200 synthetic zeolites are reported, in addition to the 40 found in nature. As mentioned previously, zeolites are an attractive option for the functional element in a sensor as they can be physically and chemically tuned to target specific analytes. A 2015 review by Wales et al highlights the wide variety of zeolites which have been applied to the sensing of gases such as carbon monoxide, nitrogen dioxide, hydrogen and VOCs among others in the automotive industry [33]. The periodic redistribution of zeolite nanoparticles within acrylate photopolymer-based volume holograms has been shown to improve the device sensitivity to gaseous VOC's such as toluene [17] and methanol [8] by providing adsorption sites for the gas molecules.

SRGs act as an ideal support structure for coatings of zeolite nanoparticles, as shown in fig. 2(a). The functionalisation of the SRG with zeolites is important to ensure sufficient localised adsorption of the gaseous analyte molecules in order to produce a measurable sensor response i.e. change in η due to variation of Δn. The Δn of the zeolite-doped grating is given by the difference between n_p and n_z, the refractive index of the zeolites. When exposed to a gaseous analyte, the analyte molecules adsorb to the porous zeolite nanoparticles as shown in fig. 2(b), resulting in a change in n_z. The overall change in Δn of the grating due to adsorption of the gas molecules to the zeolites can be determined from the change in the intensity of light diffracted by the grating. In addition to facilitating selective adsorption, by choosing zeolite nanoparticles with specific optical properties i.e. refractive index, the sensitivity and response of the SRG to gaseous analytes can be improved. Data obtained from preliminary ellipsometry measurements indicates that negligible changes in the thickness of zeolite-composite films occur during exposure to gas, implying that the surface relief amplitude, d, of SRG structures remains constant. Other options for functionalisation of surface SRG-based sensors include MIPs [42], metal organic frameworks (MOFs) [33, 43] and ionophores such as crown ethers [44].

2. Zeolite-only SRGs for gas sensing

SRGs consisting of only zeolite nanoparticles can be fabricated via lithographic and laser ablation techniques. Zeolite-only gratings are attractive for gas sensing applications as significantly larger values of Δn are possible both before and after gas exposure (fig. 3), in comparison with the zeolite-coated SRGs. The lack of a host medium also facilitates fast adsorption and desorption of gas molecules to the zeolites, which may result in faster response times and/or full sensor reversibility.

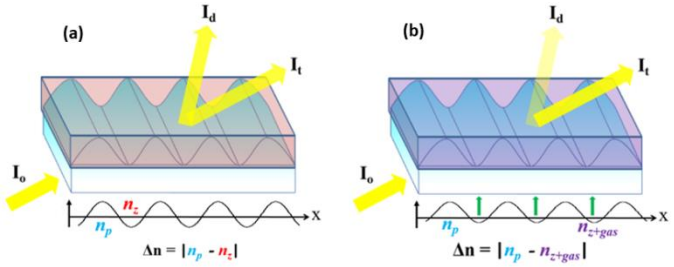

Fig. 2. Zeolite-coated SRG (a) before and (b) after gas exposure.

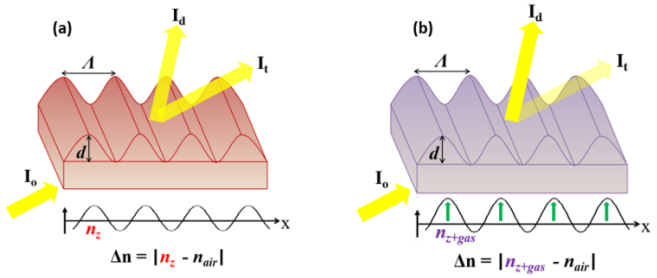

Fig. 3. Zeolite-only SRG (a) before and (b) after gas exposure.

B. Process of SRG sensor design

It is important to consider the full process of SRG sensor design from an analyte-specific view point. Fig. 4 outlines the four steps involved in sensor design and fabrication. Step 1 is to identify the target analyte, dependent on the application. Step 2 is to select a functionalising material (in this case, type of zeolite nanoparticle) that is selective for this analyte. For optimum sensor function, the smallest possible change in the initial φ or Δn of the functionalised SRG due to gas adsorption will produce a measurable change in the sensor output i.e. diffraction efficiency. For both thin and thick SRGs, an optimum initial value of Δn exists where sensor response is maximised. The type of functionalising material used will determine the initial Δn of the SRG. Based on this, step 3 of the senor design will be to determine the best platform and geometry for the SRG sensor i.e. zeolite coated or zeolite only, thin or thick. Step 4 of sensor fabrication as shown in fig. 4 is to optimise the SRG sensor physical structure i.e. SRG spatial frequency ($1/\Lambda$), surface relief amplitude (d) and reconstruction wavelength (λ_r). In this paper, steps 3 and 4 will be carried out for thin and thick SRG-based gas sensors using the theoretical model described in section 2A.

C. Description of theoretical model and equations

The sensitivity of a sensor is defined as the change in output of the sensor per unit change in the parameter being measured. For the SRG-based gas sensors under discussion here, the sensor output (i.e. grating diffraction efficiency η) is modified during gas exposure due to changes in Δn of the grating. The equations used to model the sensor output depend on the properties of the hologram itself i.e. thick or thin, surface or volume, transmission or reflection. Therefore, it is important that the holographic sensor is classified according to its thickness, design and geometry.

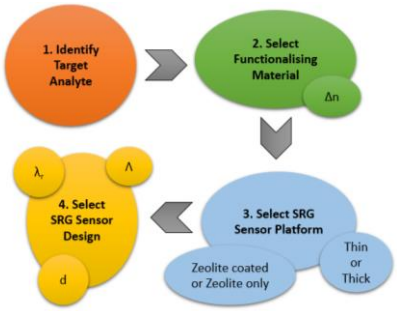

Fig. 4. Flowchart of steps involved in SRG sensor design.

The classification of diffraction gratings based on their thickness is both a well-established convention and a necessity, as thin and thick gratings exhibit different behaviour. A grating is classified as thin or thick depending on the regime of diffraction. Thin gratings are limited to a maximum diffraction efficiency of 33 % and will produce multiple diffracted waves. Thick gratings on the other hand have no limit of maximum diffraction efficiency (i.e. 100% is possible) and produce a single diffracted wave only for a Bragg angle incidence. In the literature there are two different approaches that are used to determine whether a grating operates as a thick or a thin grating. They both are derived after evaluation of the solutions of the wave equation and the amount of light transferred to the higher orders of diffraction. The Klein-Cook Q parameter [45] takes into account the physical thickness of the grating d, as well as the grating period Λ, the average refractive index n and the probe wavelength λ_r, and is described by eqn. 1a:

$$Q = \frac{2\pi\lambda_r d}{n\Lambda^2} \quad \textbf{(1a)}$$

Q values > 10 correspond to thick holograms, whereas holograms with a Q value < 1 are considered in the thin regime. Another approach proposed by Moharam and Young [46] takes into account the refractive index modulation Δn instead of the thickness d when determining the regime of operation of the grating. The ρ parameter is described by eqn.1b:

$$\rho = \frac{{\lambda_r}^2}{\Lambda^2 n\Delta n} \quad \textbf{(1b)}$$

According to the second criteria, gratings characterised by $\rho \leq 1$ are operating as thin gratings, while for $\rho > 10$ the gratings can be considered thick. When choosing the grating's parameters (spatial frequency, refractive index modulation, thickness) and probe wavelength we have ensured that both criteria are satisfied and the correct theoretical modelling approach is used. While generally speaking the two criteria classify the gratings in the same category, deviations do occur, for example for very large refractive index modulations where gratings operating typically as thick gratings (characterised by large Q factor) could produce strong multiple orders of diffraction (predicted as thin by the small ρ factor).

Two theories that are used to describe the behaviour of thin and thick gratings, and can interpreted as widely-accepted within the optics community based on their prevalence in the literature, are Raman-Nath Theory [47] and Kogenik's Coupled Wave Theory [48], respectively.

The sensor response for zeolite-coated SRGs and zeolite only SRGs has been modelled for both the thin and thick regimes. Each design has its own inherent advantages and disadvantages. The range of responses to gas of sensors based on thin SRGs is expected to be reduced in comparison to thick gratings, as the diffraction efficiency is limited to a maximum value of 33.9 % [49]. In contrast, the large surface amplitudes required for sensors based on the thick Bragg grating regime may prove difficult to produce holographically, in particular as the spatial frequency of recording is increased. However, other techniques such as laser ablation and photolithography may be effective for fabrication of surface structures with large height to period ratios. As mentioned previously, SRGs typically do not undergo changes in grating thickness due to gas adsorption at low concentrations; therefore, the sensor output has been modelled for change in Δn only.

1. Raman-Nath equations for thin gratings

Thin phase gratings, where Λ is large relative to d, exhibit Raman-Nath behaviour and produce several diffracted waves [47]. The diffraction efficiency η for thin phase gratings is given by:

$$\eta = J_m^2\left(\frac{\varphi}{2}\right) = \frac{I_d}{I_o} \quad \textbf{(2)}$$

where φ is the grating phase and m is the diffraction order. J_m is the Bessel function of the order m. The incident beam is diffracted into a number of orders, with the diffracted amplitude in the m^{th} order proportional to the value of the Bessel function. φ is defined as:

$$\varphi = \frac{2\pi\Delta n d}{\lambda_r \cos\theta_B} \quad \textbf{(3)}$$

where θ_B is the Bragg angle and λ_r is the reconstruction wavelength. For thin SRGs, the change in η relative to the change in φ due to gas adsorption has been modelled by taking the partial derivative of eqn. 2 with respect to φ:

$$\frac{\partial(\eta)}{\partial(\varphi)} = \frac{1}{2}J_1\left(\frac{\varphi}{2}\right)\left[J_0\left(\frac{\varphi}{2}\right) - J_2\left(\frac{\varphi}{2}\right)\right] \quad \textbf{(4)}$$

The change in η relative to the change in Δn due to gas adsorption is obtained by taking the partial derivative of eqn. 2 with respect to Δn:

$$\frac{\partial(\eta)}{\partial(\Delta n)} = \frac{\pi d}{\lambda_r \cos\theta_B}J_1\left(\frac{\pi d}{\lambda_r \cos\theta_B}\Delta n\right)\left[J_0\left(\frac{\pi d}{\lambda_r \cos\theta_B}\Delta n\right) - J_2\left(\frac{\pi d}{\lambda_r \cos\theta_B}\Delta n\right)\right] \quad \textbf{(5)}$$

2. Kogelnik equations for thick gratings

Thick phase gratings exhibit Bragg behaviour and produce only one diffracted beam. Maximum η is obtained when the reconstruction beam with wavelength λ_r is incident on the grating at a particular angle of incidence θ_B outside the grating given by the Bragg equation [50]:

$$\lambda_r = 2\Lambda \sin\theta_B \quad \textbf{(6)}$$

For thick holographic transmission gratings, η is defined by Kogelnik's couple wave theory [48] as:

$$\eta = \sin^2\left(\frac{\varphi}{2}\right) = \sin^2\left(\frac{\pi\Delta n d}{\lambda_r \cos\theta_B}\right) \quad \textbf{(7)}$$

The change in η relative to the change in φ due to gas adsorption for thick SRGs is found by taking the partial derivative of eqn. 7:

$$\frac{\partial(\eta)}{\partial(\varphi)} = \sin\left(\frac{\varphi}{2}\right)\cos\left(\frac{\varphi}{2}\right) \quad \textbf{(8)}$$

The change in η relative to the change in Δn is similarly given by:

$$\frac{\partial(\eta)}{\partial(\Delta n)} = \frac{\pi d}{\lambda_r \cos\theta_B}\left[\sin\left(2\frac{\pi\Delta n d}{\lambda_r \cos\theta_B}\right)\right] \quad \textbf{(9)}$$

The influence of the grating phase (φ), initial grating refractive index modulation (Δn), spatial frequency (θ_B), surface relief amplitude (d) and reconstruction wavelength (λ_r) on the sensor output (i.e. change in η) has been modelled for both thin and thick regime SRGs. From this, the optimum design for zeolite-functionalised sensors based on the SRG structure has been determined.

3. RESULTS AND DISCUSSION

The different sensor configurations which have been subjected to theoretical analysis are outlined in fig. 5. Theoretical results are presented for the sensing ability of both thin and thick SRGs which may be fabricated in media such as photopolymer or photoresist and then coated with zeolites as discussed in section 2A.1, or alternatively through fabrication of zeolite-only SRGs as described in section 2A.2.

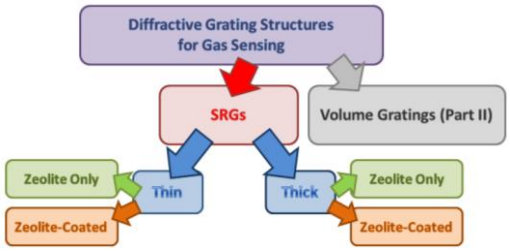

Fig. 5. Schematic of the different sensor configurations considered for theoretical modelling.

A. Modelling results for thin SRGs

The sensor response (i.e. change in η as a function of change in φ or Δn of the grating due to gas absorption) of thin zeolite-coated and zeolite only SRGs has been modelled using Raman-Nath theory as described in section 2C.1. The influence of the initial phase difference, φ, between the probe and the diffracted beams introduced by the grating, the initial grating refractive index modulation, Δn, grating spatial frequency, surface relief amplitude, d, and reconstruction wavelength, λ_r, on the SRG sensor response has been investigated in both cases. For both types of thin SRG, the experimentally achievable d is limited due to stability of the surface relief structure.

1. Initial phase difference, φ

First, let us consider the general case where the sensor output is varied due to changes in the phase difference φ as a result of gas adsorption. Fig. 6(a) shows the diffraction efficiency of a thin grating as a function of initial phase difference φ. While the ρ criterion places no restrictions on φ, the Q factor limits φ to a maximum value of 12 [45]. Due to the oscillatory nature of the Bessel function in eqn. 2, peaks and troughs corresponding to maximum (33.5%) and minimum (0%) diffraction efficiencies are observed at φ =0, 3.7, 7.7,10.7, etc. radians.

Fig. 6(b) shows the change in sensor diffraction efficiency relative to the change in φ due to gas adsorption for different values of initial phase difference introduced by the grating φ (determined by the individual grating parameters in eqn. 3), modelled using eqn. 4. When the initial phase φ value is equal to 3.7, 7.7,10.7, etc. radians, the value of $\frac{\partial(\eta)}{\partial(\varphi)}$ goes to zero, and so the change in φ required to produce a measurable change in diffraction efficiency tends to infinity. This is clearly seen in fig. 6(c), which shows the change in φ required to produce a change in diffraction efficiency of 5% for different values of initial phase difference φ. A 5% diffraction efficiency change was chosen as this is a readily measurable change in sensor readout intensity. Thus, when designing a sensor it is crucial to avoid values of φ =0, 3.7, 7.7,10.7, etc. radians, as extremely large changes in the grating phase due to gas adsorption will be required at these values in order to produce a measurable sensor response. It is noted that the 5% change in diffraction efficiency can be either positive or negative, depending on whether $\Delta\varphi$ on the y axis is increasing or decreasing with increasing φ.

2. Grating refractive index modulation, Δn

The value of grating Δn is of significant importance in holographic sensor design; it is determined by the properties of the sensor's constituent materials i.e. the relative values of n_p and n_z, as well as by the sensor configuration i.e. zeolite coated vs zeolite only. The influence of initial Δn on the sensor response to gas of thin SRGs was investigated by varying the value of Δn from 0.07 to 1 in eqn. 5, where $\Delta n = n_p - n_z$. The modelling was carried out at a spatial frequency of 500 lines/mm for four different values of d, namely 0.25, 0.5, 0.75 and 1 μm. λ_r was kept constant at 633 nm.

Fig. 7(a) shows the $\Delta(\Delta n)$ due to gas adsorption required to produce a change in η of 5% for different values of initial grating Δn. Peaks tending to infinity are clearly observed for d = 0.5, 0.75 and 1 μm. The positions of these peaks correspond to φ =0, 3.7, 7.7, etc. radians as discussed for the general case in section 3A.1. For the lowest thickness studied, d = 0.25 μm, no such peaks are observed for Δn = 0.2 – 2, as an infinity peak φ value has not yet been reached. When designing a sensor, the value of Δn will typically be fixed due to the constituent materials. Fig. 7(a) highlights the importance of careful selection of Δn and d combinations to ensure optimum gas sensor operation i.e. the lowest possible change in Δn due to gas adsorption is needed to produce a measurable change in sensor diffraction efficiency.

3. Grating spatial frequency

The effect of varying the grating spatial frequency on the sensor response of thin SRGs has been modelled using eqn. 5. This study has been carried out for four different initial values of grating Δn: 0.15, 0.3, 0.45 and 0.6. These values were chosen so as to accurately reflect different sensor configurations; for zeolite coated SRGs, lower Δn values of 0.15 (n_p=1.5; n_z=1.35/1.65) and 0.3 (n_p=1.5; n_z=1.2/1.7) are typical, whereas higher Δn values of 0.45 (n_z=1.45; n_{air}=1) and 0.6 (n_z=1.6; n_{air}=1) can be achieved for zeolite-only sensors. d = 0.5 μm and λ_r = 633 nm were used for these calculations.

Fig. 7(b) shows the $\Delta(\Delta n)$ due to gas adsorption required to produce a change in η of 5 % for different values of initial grating spatial frequency from 200-1000 lines/mm, in accordance with the Q and ρ criteria. Spatial frequencies in this range appear to be favourable for all values of Δn as a relatively flat trend in $\Delta(\Delta n)$ vs. spatial frequency is obtained. Lower spatial frequencies are preferential for fabrication of surface relief structures with high aspect ratios, as has previously been reported for acrylate-based photopolymer media [36, 37]. Thus, an optimisation study taking into consideration the ability of the material to produce the surface relief structures and the expected changes in refractive index modulation is needed at the design stage.

4. Grating surface relief amplitude, d

The effect of varying d on the sensor response of thin SRGs was then investigated. These calculations were again carried out for four different values of Δn, using λ_r = 633 nm at a spatial frequency of 500 lines/mm. This spatial frequency was selected due to the absence of infinity peaks for the range of Δn studied, as seen in fig. 6(b), which would negatively impact sensor response.

Fig. 7(c) shows the $\Delta(\Delta n)$ due to gas adsorption required to produce a 5% change in η for different values of grating d ranging from 0.1 to 1.5 μm. As previously, infinity peaks corresponding to φ =0, 3.7, 7.7, 10.7, etc. radians are repeatedly observed for Δn = 0.3, 0.45 and 0.6, highlighting again the importance of careful identification of appropriate sensor d values depending on Δn. The dependence on d is relatively flat above 0.5 μm for Δn = 0.15, therefore a larger range of surface relief amplitudes will be suitable for sensors with this initial Δn.

5. Reconstruction wavelength, λ_r

The effect of varying the value of λ_r on the sensor response of thin SRGs was modelled using eqn. 5. Only commercially available wavelengths were investigated, namely 405, 473, 532, 594, 633 and 660 nm. These calculations were carried out for four different Δn values, using d = 1 μm at 500 lines/mm. The values for d and spatial frequency were chosen based on the results obtained in sections 3A.3 and 3A.4.

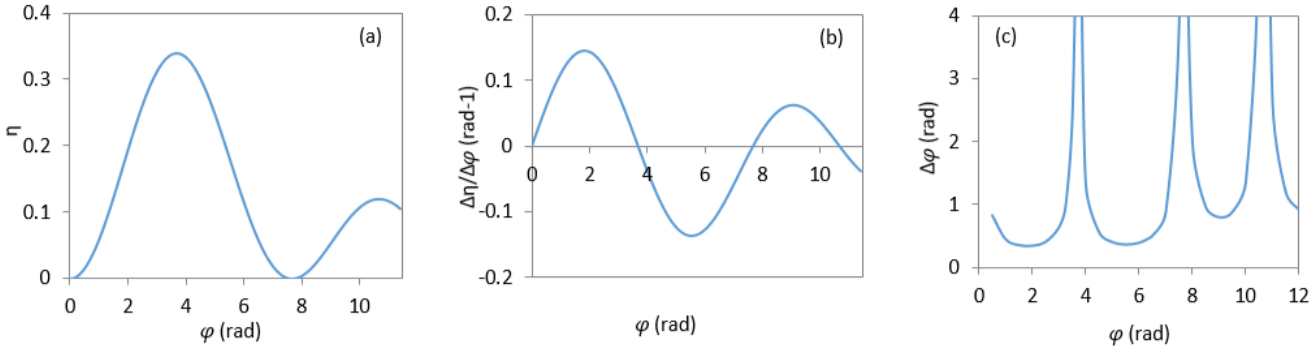

Fig. 6. For thin phase gratings: (a) diffraction efficiency v.s. φ (rad); (b) $\frac{\partial(\eta)}{\partial(\varphi)}$ vs. φ (rad); (c) the change in φ (i.e. $\Delta\varphi$) due to gas adsorption required to produce a 5% change in diffraction efficiency for different values of initial thin SRG φ.

Fig. 7(d) shows the $\Delta(\Delta n)$ due to gas adsorption required to produce a 5% change in η for different values of λ_r. It is clearly seen that for these sensor conditions, a reconstruction wavelength of 405 nm is favourable for optimum sensor response, as the smallest change in Δn due to gas exposure is required to produce a measurable change in diffraction efficiency at this wavelength. Higher λ_r of 633 and 660 nm are also favourable. It is also interesting to note that the optimum value of initial grating Δn varies depending on the value of λ_r; for 405 nm, Δn=0.15 requires a change in Δn due to gas adsorption of only 0.02 to produce a 5% change in diffraction efficiency compared to Δn = 0.45 which requires a change of 0.05. At 633 and 660 nm this trend is reversed, and sensors fabricated with Δn = 0.45 are more sensitive.

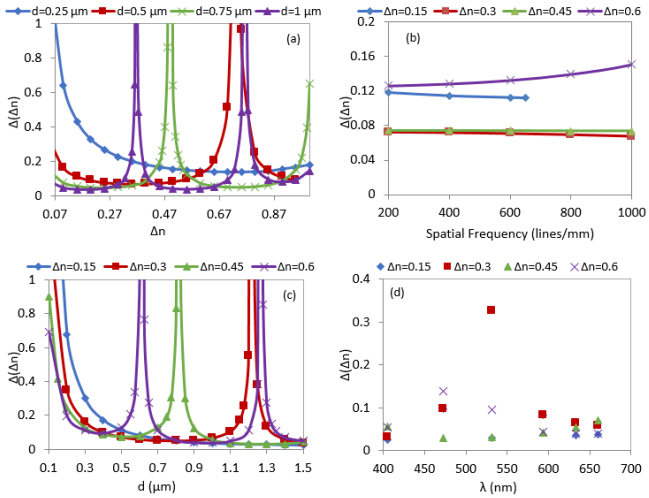

Fig. 7. $\Delta(\Delta n)$ due to gas adsorption required to produce a 5% change in diffraction efficiency for different values of initial thin SRG (a) Δn; (b) spatial frequency (lines/mm); (c) surface relief amplitude, d (μm); (d) reconstruction wavelength, λ_r (nm).

B. Modelling results for thick SRGs

The sensor response (i.e. change in η as a function of change in φ or Δn of the grating due to gas absorption) of thick zeolite-coated and zeolite only SRGs has been modelled using Kogelnik's Coupled Wave theory as described in section 2C.2. The influence of the initial grating phase, φ, initial grating refractive index modulation, Δn,, grating spatial frequency, surface relief amplitude, d, and reconstruction wavelength, λ_r, on the SRG sensor response has been investigated in both cases. As for thin SRGs, the achievable d is limited due to stability of the surface relief structure.

1. Initial phase difference, φ

Let us first consider the general case for thick SRG-based gas sensors where the sensor output is varied due to changes in the phase difference φ as a result of gas adsorption. Fig. 8(a) shows the diffraction efficiency of a thick grating as a function of initial phase difference φ. Peaks and troughs corresponding to maximum (100%) and minimum (0%) diffraction efficiencies are observed at φ =0, 3.15, 6.3, 9.45, etc. radians.

Fig. 8(b) shows the change in sensor diffraction efficiency relative to the change in φ due to gas adsorption for different values of initial phase difference introduced by the grating φ (determined by the individual grating parameters in eqn. 3), modelled using eqn. 8. Similarly to the case for thin SRGs, when the initial φ value is equal to 3.15, 6.3, 9.45, etc. radians, the value of $\frac{\partial(\eta)}{\partial(\varphi)}$ goes to zero, and so the change in φ required to produce a measurable change in diffraction efficiency tends to infinity. This is clearly seen in fig. 8(c), which shows the change in φ required to produce a change in diffraction efficiency of 5 % for different values of initial phase difference, φ. Thus, when designing a thick SRG-based sensor values of φ = , 3.15, 6.3, 9.45, etc. radians must be avoided, as extremely large changes in the grating phase difference due to gas adsorption will be required at these values in order to produce a measurable sensor response.

2. Grating refractive index modulation, Δn

The effect of initial grating Δn on the response of a thick SRG-based gas sensor was modelled using eqn. 9. The modelling was carried out at a spatial frequency of 1000 lines/mm for d = 4.5 μm; this is the minimum surface relief amplitude required for classification as a thick grating at 1000 lines/mm. It is perhaps unrealistic to expect to achieve SRGs with the necessarily large aspect ratios for classification as thick, however, for the sake of full theoretical analysis these structures will be considered. λ_r was kept constant at 633 nm.

Fig. 8(d) shows the $\Delta(\Delta n)$ due to gas adsorption required to produce a change in η of 5 % for a range of values of initial grating Δn. Peaks tending to infinity are clearly observed at approximately 0.07 and 0.13, corresponding to φ =3.15 and 6.3 radians as discussed in section 3B.1. Once again this result highlights the importance of careful selection of initial grating parameters such as Δn when designing a SRG-based sensor.

3. Grating Spatial Frequency

The effect of varying the grating spatial frequency on the sensor response of thick SRGs has been modelled using eqn. 9. As in the case of the thin SRGS, this study has been carried out for four different initial

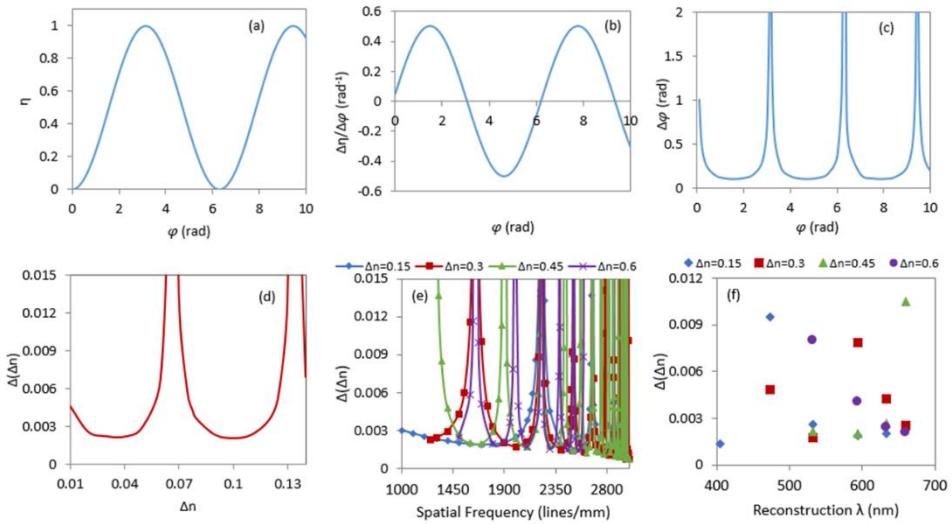

Fig. 8. For thick phase gratings: (a) diffraction efficiency vs. φ (rad); (b) $\frac{\partial(\eta)}{\partial(\varphi)}$ vs. φ (rad); (c) the change in φ (i.e. $\Delta\varphi$) due to gas adsorption required to produce a 5% change in diffraction efficiency for different values of initial thick SRG φ; (d) $\Delta(\Delta n)$ due to gas adsorption required to produce a 5% change in diffraction efficiency for different values of initial thick SRG Δn; (e)spatial frequency (lines/mm);(f) reconstruction wavelength,λ_r (nm).

values of grating Δn: 0.15, 0.3, 0.45 and 0.6 in order to describe different sensor configurations i.e. zeolite coated and zeolite only.

Fig. 8(e) shows the $\Delta(\Delta n)$ due to gas adsorption required to produce a change in η of 5 % for different values of initial thick SRG spatial frequency from 1000-3000 lines/mm. d = 4.5 μm and λ_r = 633 nm were used for these calculations. In comparison to thin SRGs, the situation is less clear, as multiple infinity peaks are present in the spatial frequency range investigated, in particular above 2000 lines/mm. Sensors fabricated with spatial frequencies close to these peaks will require very large changes in Δn due to gas adsorption in order to produce a measurable change in sensor output i.e. diffraction efficiency. Therefore, serious care must be taken when deciding on a suitable spatial frequency for fabrication of thick SRG sensors in order to avoid these peaks. For example, for Δn = 0.45 (typically a zeolite-only configuration sensor), spatial frequencies in the range of 1500-1800 lines/mm are preferable for the grating conditions modelled here.

4. Reconstruction wavelength, λ_r

The effect of varying the value of λ_r on the sensor response of thick SRGs has been modelled using eqn. 9. These calculations were carried out for four different Δn values, using d = 4.5 μm at a spatial frequency of 1500 lines/mm.

Fig. 8(f) shows the $\Delta(\Delta n)$ due to gas adsorption required to produce a 5% change in η for different values of λ_r. Once again, the trend in $\Delta(\Delta n)$ vs. reconstruction wavelength is different for each value of Δn modelled. For Δn = 0.15, 0.3, 0.45 and 0.6, optimum λ_r of 405, 532, 594 and 660 nm are calculated, respectively.

C. Discussion

The sensor response of zeolite-coated and zeolite only SRGs has been theoretically modelled for both thin and thick geometries, and the optimum conditions for fabrication as well as the maximum sensor response for each configuration are outlined in table 1.

Steps 3 and 4 of sensor design as shown in fig. 4 is to optimise the SRG sensor platform, geometry and physical structure. The theoretical modelling has identified the optimum conditions of sensor design in terms of initial grating Δn, grating spatial frequency, surface relief amplitude and reconstruction wavelength for both thin and thick SRGs. The theoretical modelling has shown that in certain cases, both spatial frequency and d should be as high as possible for optimum sensor response; however, realistically achievable values for SRG structures are shown in Table 1 for the sake of practicality.

Table 1. Summary of sensor response for different SRG configurations

	Δn	*Spatial Frequency (lines/mm)*	d *(μm)*	λ_r *(nm)*	*Sensor response i.e.* $\Delta(\Delta n)$ *for* $\Delta\eta$ = 1%
Thin	0.15	500*	1*	405	4.9×10^{-3}
	0.3			405	6.2×10^{-3}
	0.45			473	6.4×10^{-3}
	0.6			660	7.8×10^{-3}
Thick	0.15	1500*	4.5*	405	2.7×10^{-4}
	0.3			532	3.5×10^{-4}
	0.45			594	4.1×10^{-4}
	0.6			660	4.2×10^{-4}

*Value, while not theoretically optimum, is potentially achievable for SRGs

The thick SRG-based sensors are an order of magnitude more sensitive to changes in Δn due to gas adsorption, with $\Delta(\Delta n)$ due to gas adsorption in the order of 10^{-4} required to produce a 1 % change in diffraction efficiency in comparison to 10^{-3} for thin SRG-based sensors for the same values of initial Δn. A contributing factor to this is the difference in spatial frequency and surface relief amplitude between the thin and thick SRG configurations. This is due to the restrictions imposed on SRGs in order to be classified as "thick", from eqn. 1a, i.e. a minimum d of 4.5 μm is required at 1000 lines/mm, whereas no such restrictions are in place for thin SRGs. The likelihood of fabricating thick SRGs with such high aspect ratios in currently available polymers and photoresists is low, however, thin SRGs are readily producible. This results reveal a trend towards higher sensitivity in thick gratings and since experimentally the fabrication of pure thick (volume) gratings is currently not achievable, gratings operating in intermediate regime 1<Q<10, should also be considered in the future.

From table 1 it can also be concluded that the zeolite-coated SRGs (Δn=0.15, 0.3) are on average more sensitive than the zeolite only SRGs (Δn=0.45, 0.6) for both thin and thick geometries. This implies that

lower values of initial grating Δn are in fact favourable for SRG sensor design.

A main conclusion from the study is that the reconstruction wavelength used for sensor readout has a significant impact on the sensitivity of the sensor system. This difference may be explained by considering the relative sizes of Δn and d (i.e. φ), which play a significant role due to the oscillatory nature of the Bessel and Sine functions in eqns. 5 and 9 for thin and thick SRGs, respectively. For example, for a 4.5 μm thick SRG sensor with initial Δn = 0.3 and spatial frequency = 1500 lines/mm, the change in Δn due to gas adsorption required to produce a 1 % change in diffraction efficiency is reduced by two orders of magnitude from 3×10^{-2} to 3.5×10^{-4} as λ_r is increased from 405 nm to 532 nm. However, if the initial Δn of this SRG-based sensor is increased to 0.45, then the required change in Δn due to gas adsorption is reduced from 2.1×10^{-3} to 4.1×10^{-4} as λ_r is reduced from 660 nm to 594 nm. Therefore, there is no single optimum λ_r for SRG-based sensors as this depends greatly on the individual initial SRG parameters. The selection of the probe wavelength λ_r for sensor readout requires careful consideration of the initial grating parameters if sensor response is to be maximised.

4. CONCLUSIONS

The suitability of SRG structures recorded in zeolite composite materials for gas sensing applications has been investigated. Theoretical modelling of the response of different sensor designs was carried out using both the Raman-Nath and Kogelnik's Couple Wave theories. The influence of a range of parameters on the sensor response of both thin and thick regime SRGs has been studied, namely phase difference introduced by the grating, refractive index modulation, spatial frequency, surface relief amplitude and reconstruction wavelength. From this, the optimum fabrication conditions for both thin and thick regime SRG-based gas sensors have been identified. The importance of first carrying out theoretical modelling in the design and fabrication of holographic grating-based sensors has been highlighted.

Part 2 of this paper will focus on the theoretical design of volume-based holographic structures for gas sensing. Sensors based on volume gratings are not restricted by surface relief amplitude and spatial frequency in the same way as SRGs, as they can readily record up to 100 % diffraction efficiency gratings in significantly thicker layers, resulting in improved sensor response due to gas adsorption. An additional advantage of volume sensors is that they can be fabricated in reflection mode, allowing for visual readout via a colour change in the presence of a gas. For volume-based sensors it is necessary to consider simultaneous changes in both Δn and d as both will occur due to gas adsorption to the zeolites. This is particularly an issue for reflection mode sensors; a 0.005 μm change in grating thickness will produce a 10 nm change in reconstruction wavelength. A thorough analysis of the volume grating sensor response due to changes in both Δn and d is presented.

Funding information. Dublin Institute of Technology's Arnold F Graves Postdoctoral Fellowship Programme.

References:

1. J. Hodgkinson and R. P. Tatam, "Optical gas sensing: a review", Meas. Sci. Technol. **24**, 012004 (2013).
2. H. Bai and G. Shi, "Gas Sensors Based on Conducting Polymers", Sensors **7**(3), 267-307 (2007).
3. A. M. Azad, S. A. Akbar, S. G. Mhaisalkar, L. D. Birkefeld, and K. S. Goto, "Solid-State Gas Sensors: A Review", J. Electrochem. Soc. **139**(12), 3690-3704 (1992).
4. G. Eranna, B. C. Joshi, D. P. Runthala, and R. P. Gupta, "Oxide Materials for Development of Integrated Gas Sensors—A Comprehensive Review", Crit. Rev. Solid State **29**(3-4), 111-188 (2004).
5. Y. Wang and J. T. W. Yeow, "A Review of Carbon Nanotubes-Based Gas Sensors", Journal of Sensors, 2009, 1-24 (2009).
6. Transparency Market Research, "Gas Sensors Market - Global Industry Size, Share, Trends, Analysis and Forecast, 2012 - 2018", July 2013. Available online at: http://www.transparencymarketresearch.com/gas-sensors-market.html [Accessed: 15-08-2017].
7. Grand View Research, "Gas Sensors Market Analysis And Segment Forecasts To 2020", March 2014. Available online at: http://www.grandviewresearch.com/industry-analysis/gas-sensors-market [Accessed: 15-08-2017].
8. M. Zawadzka, T. Mikulchyk, D. Cody, S. Martin, E. Mihaylova, A. K. Yetisen, J. L. Martinez-Hurtado, H. Butt, H. Awala, S. Mintova, S. H. Yun, I. Naydenova, "Photonic Materials for Holographic Sensing" in "Photonic Materials for Sensing, Biosensing, and Display Devices", Springer (2015).
9. A. G. Mayes, J. Blyth, M. Kyröläinen-Reay, R. B. Millington, and C. R. Lowe, "A holographic alcohol sensor", Anal. Chem. **71**(16), 3390–3396 (1999).
10. S. Kabilan, J. Blyth, M. C. Lee, A. J. Marshall, A. Hussain, X.-P. Yang and C. R. Lowe, "Glucose-sensitive holographic sensors", J. Mol. Recogn. **17**(3), 162–166 (2004).
11. B. M. González, G. Christie, C. A.B. Davidson, J. Blyth, and C.R. Lowe, "Divalent metal ion-sensitive holographic sensors", Anal. Chim. Acta **528**(2), 219–228 (2005).
12. A. J. Marshall, J. Blyth, C. A. B. Davidson, and C. R. Lowe, "pH-sensitive holographic sensors", Anal. Chem. **75**(17), 4423–4431 (2003).
13. T. Mikulchyk, S. Martin, and I. Naydenova "Humidity and temperature effect on properties of transmission gratings recorded in PVA/AA-based photopolymer layers", J. Opt. **15**(10), 105301 (2013).
14. C. R. Lowe, J. Blyth, and A. P. James, "Interrogation of a sensor", US 20080094635 A1 (2008).
15. E. Mihaylova, D. Cody, I. Naydenova, S. Martin, and V. Toal, "A Holographic Recording Composition", WO2016001108 A1.
16. I. Naydenova, J. Raghavendra, V. Toal, and S. Martin, "A Visual Indication of Environmental Humidity using a Color Changing Hologram Recorded in a Self-developing Photopolymer", Appl. Phys. Lett. **92**, 031109 (2008).
17. E. Leite , I. Naydenova, S. Mintova, L. Leclercq, and V. Toal, "Photopolymerisable Nanocomposites for Holographic Recording and Sensor Application", Appl. Opt. **49**(19), 3652-3660 (2010).
18. D. Yu, H. Liu, D. Mao, Y. Geng, W. Wang, L. Sun and J. Lv, "Enhancement of spectrum strength in holographic sensing in nanozeolites dispersed acrylamide photopolymer", Opt. Express 23(22), 29113-29126 (2015).
19. D. Mao, Y. Geng, H. Liu, K. Zhou, L. Xian, and D. Yu, "Two-way shift of wavelength in holographic sensing of organic vapor in nanozeolites dispersed acrylamide photopolymer", Appl. Opt. 55(23), 6212-6221 (2016).
20. J. L.. Martínez-Hurtado, C. A. Davidson, J. Blyth, and C. R. Lowe, "Holographic detection of hydrocarbon gases and other volatile organic compounds", Langmuir **26**(19), 15694–15699 (2010).
21. V. K. S. Hsiao, W. D. Kirkey, F. Chen, A. N. Cartwright, P. N. Prasad, and T. J. Bunning, "Organic Solvent Vapor Detection Using Holographic Photopolymer Reflection Gratings" Adv. Mater. **17**(18), 2211–2214 (2005).
22. Y. Fuchs, S. Kunath, O. Soppera, K. Haupt, and A. G. Mayes, "Molecularly imprinted silver-halide reflection holograms for label-free opto-chemical sensing", Adv. Funct. Mater. **24**, 688 (2014).

23. Y. Fuchs, O. Soppera, A. G. Mayes, and K. Haupt, “Holographic molecularly imprinted polymers for label-free chemical sensing”, Adv. Mater. **25**, 566 (2013).
24. J. J. Cowan, “Aztec surface-relief volume diffractive structure”, J. Opt. Soc. Am. A **7**, 1529 (1990).
25. J. J. Cowan, “Advances in holographic replication with the Aztec structure”, Proceedings of the 7th International Symposium on Display Holography, Wales, UK (2006).
26. D. S. Hobbs, “Laser damage threshold measurements of microstructure-based high reflectors” Proceedings of the 2008 Laser-Induced Damage in Optical Materials, **7132**, Boulder, CO, (2008).
27. J. J. Cowan, “The Aztec structure: an improved replicable security device”, *Proc. SPIE* 6075, Optical Security and Counterfeit Deterrence Techniques VI, 60750Q (2006).
28. A. K. Yetisen, I. Naydenova, F. da Cruz Vasconcellos, J. Blyth, and C. R. Lowe, “Holographic sensors: three-dimensional analyte-sensitive nanostructures and their applications”, Chem. Rev. **114**(20), 10654-96 (2014).
29. A. K. Yetisen, H. Butt, T. Mikulchyk, R. Ahmed, Y. Montelongo, M. Humar, N. Jiang, S. Martin, I. Naydenova, and S. Hyun Yun, “Color-Selective 2.5D Holograms on Large-Area Flexible Substrates for Sensing and Multilevel Security”, Adv. Optical Mater. **4**(10), 1589-600 (2016).
30. T. Mikulchyk, “Development of Holographic Sensors for Monitoring Relative Humidity and Temperature”, Doctoral Thesis, Dublin Institute of Technology, 2016.
31. J. L. Martinez Hurtado and C.R. Lowe, “An integrated photonic-diffusion model for holographic sensors in polymeric matrices” J. Membr. Sci. **495**(1), 14-19 (2015).
32. Hongpeng Liu, Dan Yu, Dongyao Mao, Yaohui Geng, Weibo Wang “Modeling swelling and absorption dynamics for holographic sensing in analytes sensitive photopolymer” Opt. Comm. **368**, 95–104, (2016).
33. D. J. Wales, J. Grand, V. P. Ting, R. D. Burke, K. J. Edler, C. R. Bowen, S. Mintova, and A. D. Burrows “Gas sensing using porous materials for automotive applications” Chem. Soc. Rev. **44**, 4290 (2015).
34. K. Sahner, G. Hagen, D. Schönauer, S. Reiß, and R. Moos, “Zeolites — Versatile materials for gas sensors”, Solid State Ionics **179**(4), 2416–2423 (2008).
35. Xiaowen Xu,Jing Wang, and Yingcai Long, “Zeolite-based Materials for Gas Sensors”, Sensors **6**(12), 1751-1764 (2006).
36. Y. Boiko, V. Slovjev, S. Calixto, and D. Lougnot, “Dry photopolymer films for computer-generated infrared radiation focusing elements,” Appl. Opt. **33**, 787-793 (1994).
37. C. Croutxe-Barghorn and D. Lougnot, “Use of self-processing dry photopolymers for the generation of relief optical elements: a photochemical study”, Pure Appl. Opt. **5**, 811-825 (1996).
38. I. Naydenova, E. Mihaylova, S. Martin, and V. Toal, “Holographic patterning of acrylamide–based photopolymer surface”, Opt. Express, **13**(13), 4878-4889 (2005).
39. K. Trainer, K. Wearen, D. Nazarova, I. Nadenova, and V. Toal, “Optimisation of an acrylamide-based photopolymer system for holographic inscription of surface patterns with sub-micron resolution”, J. Opt. **12**, 124012 (2010).
40. Won-Tien Tsang and Shyh Wang, “Simultaneous exposure and development technique for making gratings on positive photoresist” Appl. Phys. Lett. **24**, 196 (1974).
41. M. Yan and A. Kapua, “Fabrication of molecularly imprinted polymer microstructures”, Anal. Chim. Acta **435**(1), 163–167 (2001).
42. Y. Fuchs, O. Soppera, and K. Haupt, “Photopolymerization and photostructuring of molecularly imprinted polymers for sensor applications—A review”, Anal. Chim. Acta 717, 7-20 (2012).
43. V. Pentyala, P. Davydovskaya, M. Ade, R. Pohle, and G. Urban, “Metal–organic frameworks for alcohol gas sensor”, Sens. Actuators, B **222**, 904-909 (2016).
44. A. Giovannitti , C. B. Nielsen , J. Rivnay , M. Kirkus , D. J. Harkin , A. J.P. White , H. Sirringhaus , G. G. Malliaras , and I. McCulloch, “Sodium and Potassium Ion Selective Conjugated Polymers for Optical Ion Detection in Solution and Solid State” Adv. Funct. Mater. **26**, 514–523 (2016).
45. W. R. Klein and B. D. Cook, “Unified approach to ultrasonic light diffraction”, IEEE Transactions on Sonics and Ultrasonics **14**(3), 123 - 134 (1967).
46. M.G. Moharam and L. Young, “Criterion for Bragg and Raman-Nath diffraction regimes”, Appl. Opt. **17** (11), 1757-1759 (1978).
47. C. V. Raman and N. S. Nagendra Nath, “The diffraction of light by high frequency sound waves: Part I” in Proc. Indian Acad. Sci. A 2 406-412 (1935).
48. H. Kogelnik, “Coupled wave theory for thick hologram gratings”, The Bell System Technical Journal 48(9), 2909-2947 (1969).
49. P. Hariharan, Optical Holography: Principles, Techniques and Applications, Cambridge University Press, 1984.
50. W. L. Bragg "The Diffraction of Short Electromagnetic Waves by a Crystal", Proceedings of the Cambridge Philosophical Society **17**, 43–57 (1913).